

ANL/CP--73766

11

DE91 016518

SUB-BARRIER FUSION
AN EXPERIMENTAL REVIEW

R. R. Betts
Physics Division
Argonne National Laboratory
Argonne, IL 60439
USA

DISCLAIMER

This report was prepared as an account of work sponsored by an agency of the United States Government. Neither the United States Government nor any agency thereof, nor any of their employees, makes any warranty, express or implied, or assumes any legal liability or responsibility for the accuracy, completeness, or usefulness of any information, apparatus, product, or process disclosed, or represents that its use would not infringe privately owned rights. Reference herein to any specific commercial product, process, or service by trade name, trademark, manufacturer, or otherwise does not necessarily constitute or imply its endorsement, recommendation, or favoring by the United States Government or any agency thereof. The views and opinions of authors expressed herein do not necessarily state or reflect those of the United States Government or any agency thereof.

Invited Paper Present at International Symposium: "Towards a Unified Picture of Nuclear Dynamics", June 6-8, 1991 Nikko, Japan.

MASTER

DISTRIBUTION OF THIS DOCUMENT IS UNLIMITED

ps

The submitted manuscript has been authored by a contractor of the U. S. Government under contract No. W-31-109-ENG-38. Accordingly, the U. S. Government retains a nonexclusive, royalty-free license to publish or reproduce the published form of this contribution, or allow others to do so, for U. S. Government purposes.

SUB-BARRIER FUSION - AN EXPERIMENTAL REVIEW

R. R. Betts

Physics Division, Argonne National Laboratory, Argonne, IL 60439*

ABSTRACT

This paper contains a review of the current status of the experimental study of heavy-ion fusion at sub-barrier energies. Emphasis is placed on the comparison of the experimentally observed quantities with theoretical expectations. Results of measurements of the spin distributions of the composite systems formed following fusion are critically examined with a view to understanding the large discrepancies between theory and experiment which exist for some systems.

INTRODUCTION

Fusion of heavy ions at energies in the vicinity of the classical barrier has been actively studied for the last decade. The observation which sparked this tremendous activity having been the initial observation^{1,2} of cross-sections at sub-barrier energies far in excess of those predicted by simple models. The physics underlying these observations has been known in a general way for quite some time, namely, quantum tunneling of the two ions in the presence of couplings to other degrees of freedom. Nevertheless, there continue to exist significant discrepancies between experiment and theory which act as a stimulus for further investigation. The basic physics to be studied via sub-barrier fusion is one of general application which appears in many other areas of physics. For example, tunneling phenomena are abundant in condensed matter studies and the role of coupling to other degrees of freedom in enhancing barrier penetration is strikingly obvious in the case of catalysis of chemical reactions.

The nuclear case, studied via heavy ion fusion is a rich field. The variety of nuclear shapes and other collective degrees of freedom which can be varied at will by suitable choice of target and projectile allows systematic study of the influence of changing couplings vice-versa, it is possible that we may gain new insight into the properties of the dinuclear system itself through the application of these studies.

CROSS SECTIONS

The first observation of enhanced cross-sections for sub-barrier fusion were reported by Stokstad et al.¹ for $^{16}\text{O} + \text{Sm}$. These data, augmented by data for isotopes not measured in the original work³ are shown in Fig. 1. The results are well-known; a progression towards higher cross-section in the sub-barrier region is seen to occur for increasing target mass, correlated with the transition from spherical ^{144}Sm to well deformed ^{154}Sm . The curves shown superimposed on the data are the results of a calculation

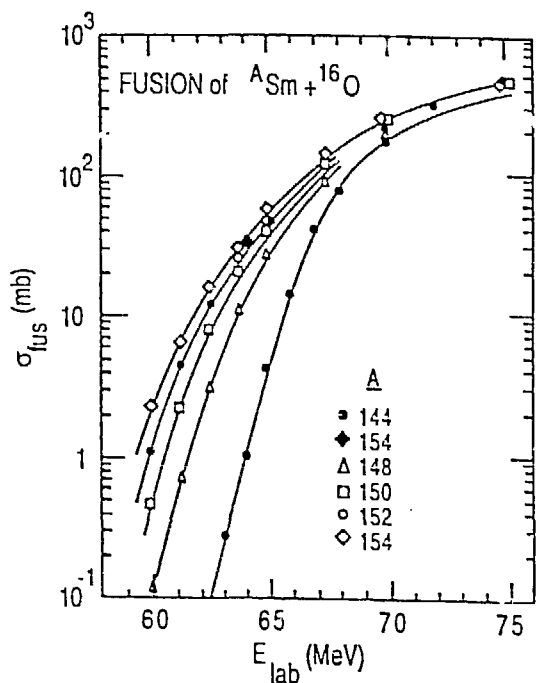


Fig. 1. Fusion cross-sections for ${}^{16}\text{O} + \text{Sm}$. The solid curves are fits to the data using the model of Wong.

using a model due to Wong⁴ in which the barrier between the two ions is modified by the static deformation of the target nucleus, increased deformation resulting in an overall lowering of the barrier when averaging of the (random) orientations of the target nucleus is taken into account. More sophisticated models (coupled-channels) in which the coupling between the entrance channel and inelastic channels is handled quantum-mechanically are also able to account for the observed cross-sections for these systems. This approach has the further merit that couplings to inelastic channels not represented by static ground-state deformation can also be included. Thus, even for spherical target and projectile nuclei, the sub-barrier fusion is enhanced due to barrier fluctuations introduced by the coupling to strong quadrupole and octupole vibrational excitations. This is demonstrated by data for Ni + Ni due to Beckerman et al.² shown together with a variety of calculations in Fig. 2. The solid lines are the results of coupled channels calculations by Esbensen and Landowne⁵ in which all inelastic couplings of the one- and two-phonon excitations of target and projectile were included. For the symmetric ${}^{58}\text{Ni} + {}^{58}\text{Ni}$ and ${}^{64}\text{Ni} + {}^{64}\text{Ni}$ systems, the agreement is excellent. Large discrepancies were found for the ${}^{58}\text{Ni} + {}^{64}\text{Ni}$ system however. It was suspected for some time that this discrepancy might arise from a neglect of neutron transfer channels which, for the asymmetric system, have well-matched Q-values. Inclusion of these channels in the calculation⁶ leads to an improvement in the agreement, although still worse than the symmetric cases. This same calculation also shows good agreement with the measured⁷ neutron transfer cross-sections as shown in Fig. 3. It should not be forgotten that

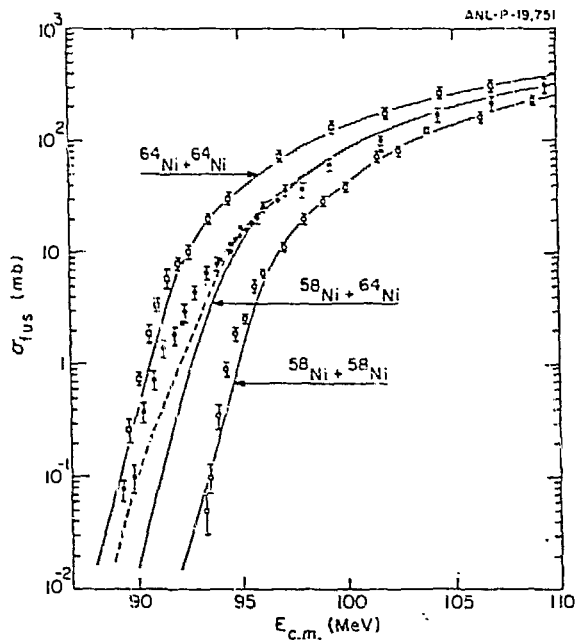


Fig. 2. Fusion cross-sections for Ni + Ni isotopes. The solid curves are coupled channels calculations including one- and two-phonon vibrational excitations. The dashed curve shows the effect of including one- and two-neutron transfer channels.

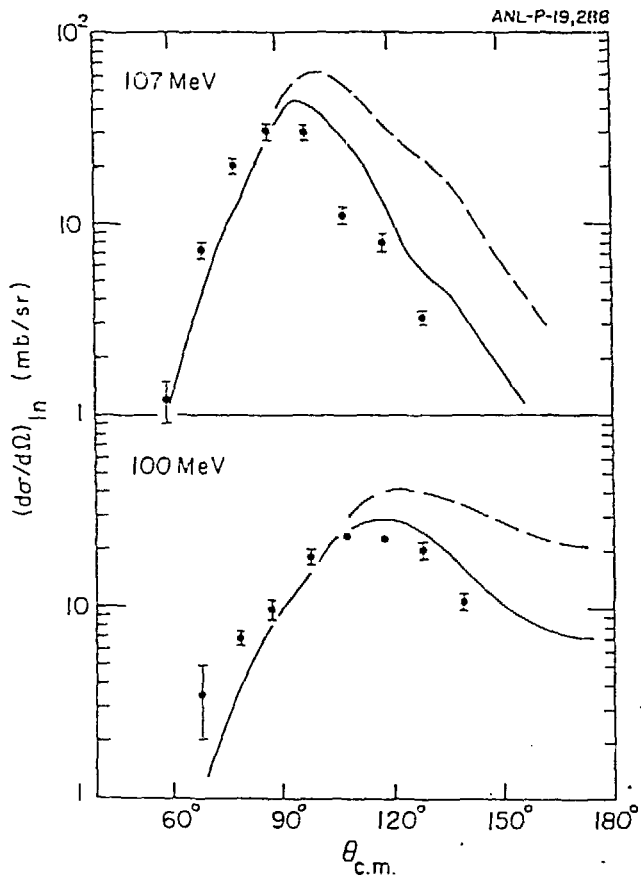


Fig. 3. Angular distributions for one-neutron transfer in the $^{58}\text{Ni} + ^{64}\text{Ni}$ system. The curves show the results of coupled channels calculations with (solid) and without (dashed) the inclusion of second-step neutron transfer.

coupled-channels theories of fusion must also give a good description of the reaction channels themselves and care should be taken to ensure that a good description of the fusion channel is not obtained at the expense of some other important channel.

An interesting aspect of the data is demonstrated in Fig. 4

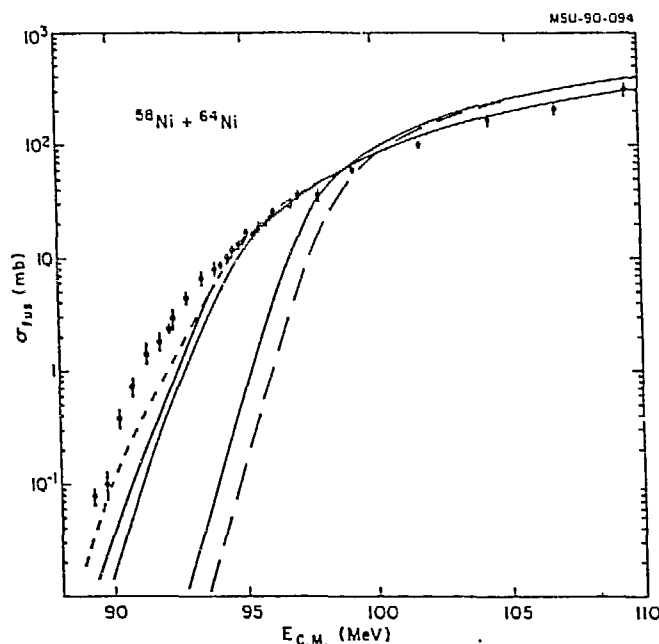


Fig. 4. Data for $^{58}\text{Ni} + ^{64}\text{Ni}$ fusion. The lower dashed curve is the no-coupling limit. Note the above barrier suppression in comparison with this limit and the correct description of the data by the coupled-channels calculations both above and below the barrier.

where the effects of including different couplings on the calculated cross-sections is shown in comparison with the data for $^{58}\text{Ni} + ^{64}\text{Ni}$. In addition to the couplings producing an enhancement at sub-barrier energies, we see that these same couplings produce a suppression of the fusion in the energy region immediately above the barrier. Thus, reaction channels which are strong above the barrier and there deplete the fusion channel are responsible for enhancements in the sub-barrier region. A more graphic demonstration of this feature of fusion cross-sections is found in data⁸ for much heavier systems shown in Fig. 5. In this case, the measured evaporation residue cross-sections have been translated into a "Fusion Probability" by correcting the data for fission decay of the compound nucleus using statistical model calculations and by assuming an ℓ -independent probability for fusion. It is striking to see again the suppression of fusion relative to the expectations of either the Bass Model (dotted curves) or calculations with barriers shifted to account for the lowest energy data (dashed curves). The strong dependence of the suppression on the exact nuclear system is suggestive of the influence of nuclear structure, perhaps due to shell effects in the di-nuclear system⁹ or to dissipation in the approach phase leading

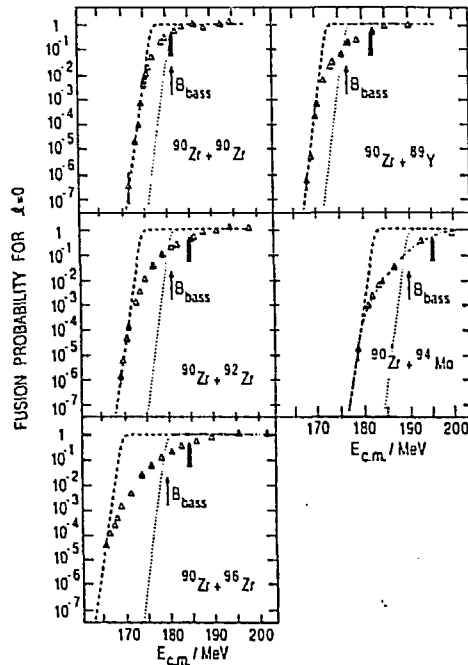


Fig. 5. Fusion probabilities for heavy symmetric systems showing, when compared with no-coupling calculations using the Bass model (dotted curve), the above barrier suppression and below barrier enhancement.

to strongly damped or deep-inelastic processes which compete with fusion. For these very heavy systems, the coupled channels approach fails due to the large number of complex reaction channels which are open. It is nevertheless a challenge to find a theoretical link which will allow the understanding of all the data on a common footing.

SPIN DISTRIBUTIONS

Although the cross-sections for fusion and other reaction channels are the first quantities which must be accounted for by any theory, it is clear that these may not distinguish between different models. For example, it has been argued¹⁰ that an energy dependent potential derived from the elastic scattering channel may give a good account of sub-barrier fusion cross-sections. It was subsequently pointed out¹¹ that such an approach leads to a different prediction for the spin distribution of the fused system than does a full coupled-channels calculation. The motivation for attempting such measurements is therefore clear. Three different techniques have so far been employed to gain information on the spin distributions; isomer ratios, gamma-ray multiplicities and fission fragment angular distributions. The first and last methods have been used to provide information on the mean or r.m.s. value of the fused system whereas the measurement of gamma-ray multiplicities can, in principle, give much more detailed information on the distribution of angular momenta.

Isomer Ratios: DiGregorio et al. have measured the relative population of the ground ($J^\pi=3/2^+$) and isomeric ($J^\pi=11/2^-$) states in ^{137}Ce with projectiles ranging from ^3He to ^{12}C . Due to the large difference in spin between these two states, their population originates from different regions of spin in the decaying compound nucleus and the ratio of their population is therefore sensitive to the spin distribution. The deduced mean spins obtained by this method are in good agreement with coupled-channels predictions over a range of energies near the barrier. These results are summarized in Fig. 6.

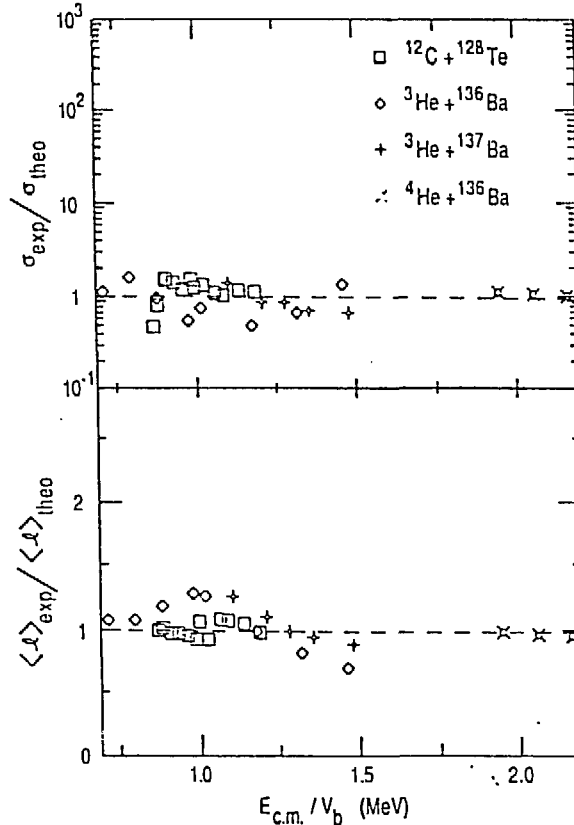


Fig. 6. Comparison of experimental and theoretical cross-sections and average angular momenta for systems measured using the isomer ratio technique.

Gamma Multiplicities: Measurements of this type can be divided into two categories. Those using a relatively small number of gamma-ray detectors and those using highly-segmented 4π arrays. A number of measurements using the former technique have been carried out by Vandenbosch, Gil and collaborators. Evaporation residues were identified either by detection of characteristic gamma-rays with a high-resolution detector or using a charged particle detector in conjunction with an electrostatic deflector to detect evaporation residues directly. Data for a variety of projectiles; α , ^{12}C , ^{16}O and ^{28}Si incident on ^{154}Sm have been used to deduce the mean angular momentum of the decaying compound nucleus^{13,14} as a function of bombarding energy. These data are shown in Figs. 7 and 8 in comparison with calculated values from the model of Wong⁴. The overall agreement is impressively good.

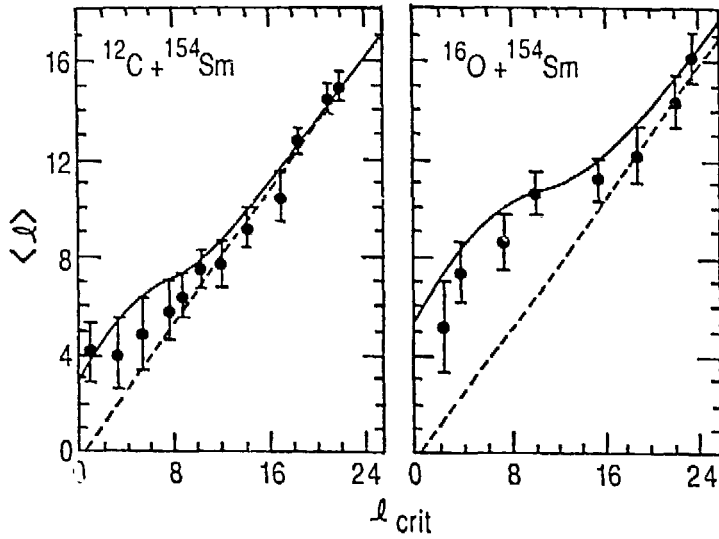


Fig. 7. Average angular momenta deduced from gamma-ray multiplicities for the $^{12}\text{C} + ^{154}\text{Sm}$ and $^{16}\text{O} + ^{154}\text{Sm}$ systems shown in comparison with no-coupling (dashed) and Wong model (solid) calculations.

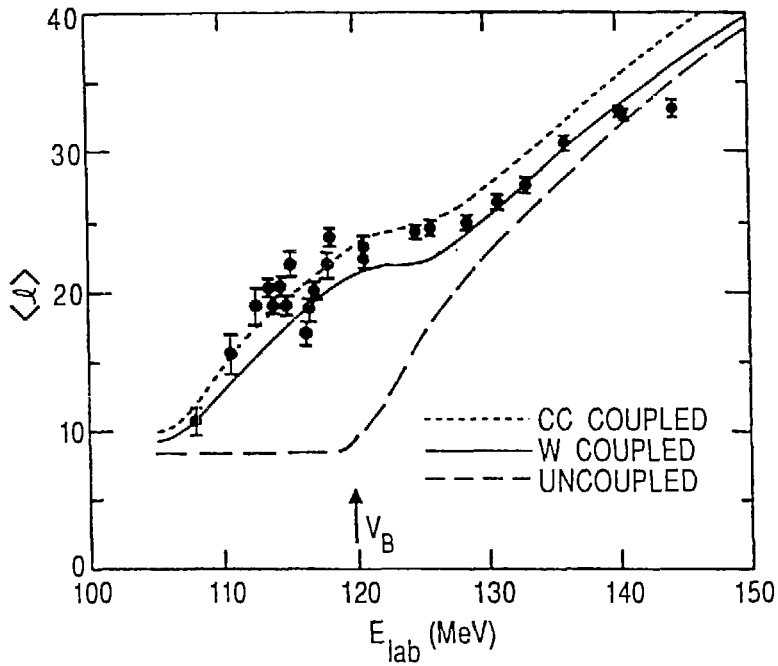


Fig. 8. Average angular momenta deduced from gamma-ray multiplicities for $^{28}\text{Si} + ^{154}\text{Sm}$ shown in comparison with no-coupling (dashed), Wong (solid) and coupled-channels (short dashed) model calculations.

The good agreement between experiment and theory found for the above studies is not however universal. A summary of essentially all the published gamma-ray multiplicity data as compiled in Ref. 12 is shown in Fig. 9. Two notable exceptions to the overall good

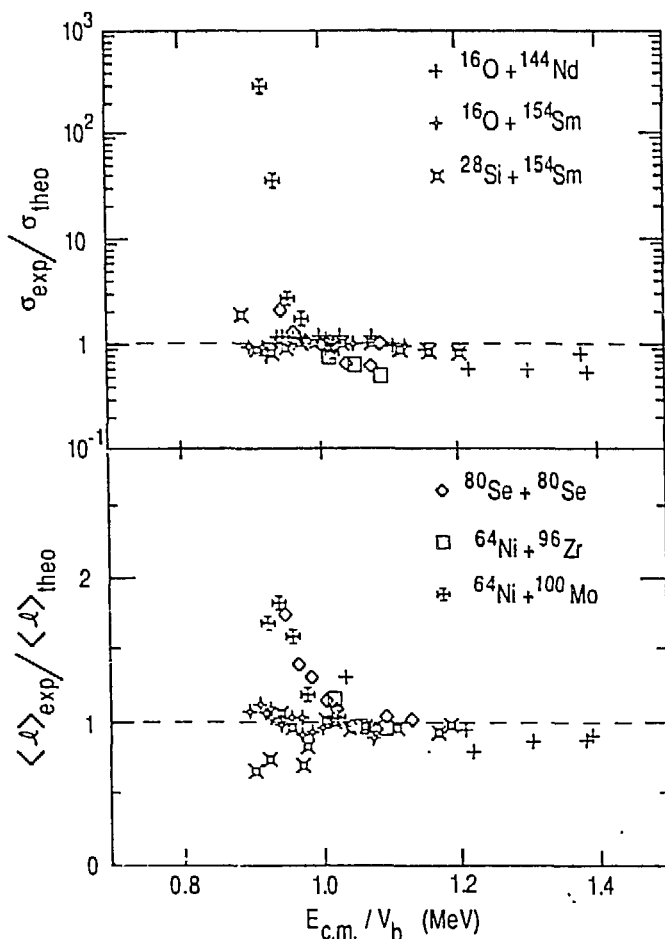


Fig. 9. Comparison of experimental and theoretical cross-sections and angular momenta for systems measured using gamma-ray multiplicities. Note the large values for $^{80}\text{Se} + ^{80}\text{Se}$ and $^{64}\text{Ni} + ^{100}\text{Mo}$.

agreement are seen - $^{80}\text{Se} + ^{80}\text{Se}$ ¹⁵ and $^{64}\text{Ni} + ^{100}\text{Mo}$ ¹⁶. Concentrating on the $^{64}\text{Ni} + ^{100}\text{Mo}$ case - which is the more complete experiment and analysis of the two - we see that the coupled-channels calculation fails to predict both the experimental cross-sections and mean spin in the sub-barrier region. Even when the inelastic coupling strengths are arbitrarily increased by 50% to account for the sub-barrier cross-section, the mean and r.m.s. spins are still underpredicted in the sub-barrier region as shown in Fig. 10. This result therefore may represent a very significant discrepancy between theory and experiment.

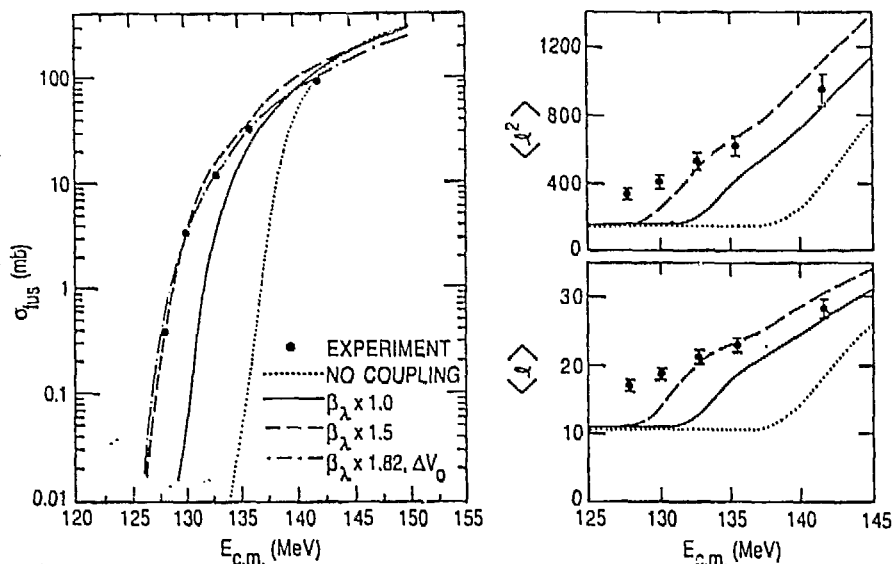


Fig. 10. Cross-sections and mean angular momenta for the $^{64}\text{Ni} + ^{100}\text{Mo}$ system. The curves show the results of various calculations identified in the figure.

It is therefore important to critically examine the experimental method and analysis in this and the $^{80}\text{Se} + ^{80}\text{Se}$ cases. Both experiments employ the same technique, namely, a large array of NaI ($^{64}\text{Ni} + ^{100}\text{Mo}$) or BGO ($^{80}\text{Se} + ^{80}\text{Se}$) detectors, used in conjunction with Ge detectors with which evaporation residues are identified by their characteristic discrete lines. Fold or hit distributions in the array for the various evaporation channels are thus obtained by gating on the discrete lines in the Ge detectors. In order that the weak evaporation channels can be seen in the presence of much more intense Coulomb excitation and transfer channels, the low folds must be suppressed electronically. Although this is corrected for in the analysis, it is possible that a bias towards higher folds is thus placed on the data. Another possible experimental difficulty comes from the relative weakness of the fusion gamma rays which may result in the missing of weak channels and also necessitates background subtraction to obtain clean fold distributions. Finally, in the analysis of these data, a unique transformation from gamma-ray multiplicity to spin was used when it is clear that the relation must depend on spin, especially at low values of the spin.

To overcome these difficulties, we have recently carried out measurements¹⁷ of $^{160}\text{Gd} + ^{152}\text{Sm}$ fusion using a high efficiency system to directly detect evaporation residues in conjunction with a 42 element BGO array (70% of 4π) also surrounded by 8 Compton-suppressed Ge detectors. The evaporation residue detector consisted of a 25 element silicon array downstream of an electrostatic deflector. This system provides effective suppression of scattered beam particles while giving an overall detection efficiency of approximately 20% for evaporation residues. At an energy where the fusion cross-section is only 1 mb (5 MeV below the barrier), excellent statistics data were obtained in only two hours running.

Data were obtained at five energies between 60 and 80 MeV. The experimental fold distributions are shown in Fig. 11. These fold

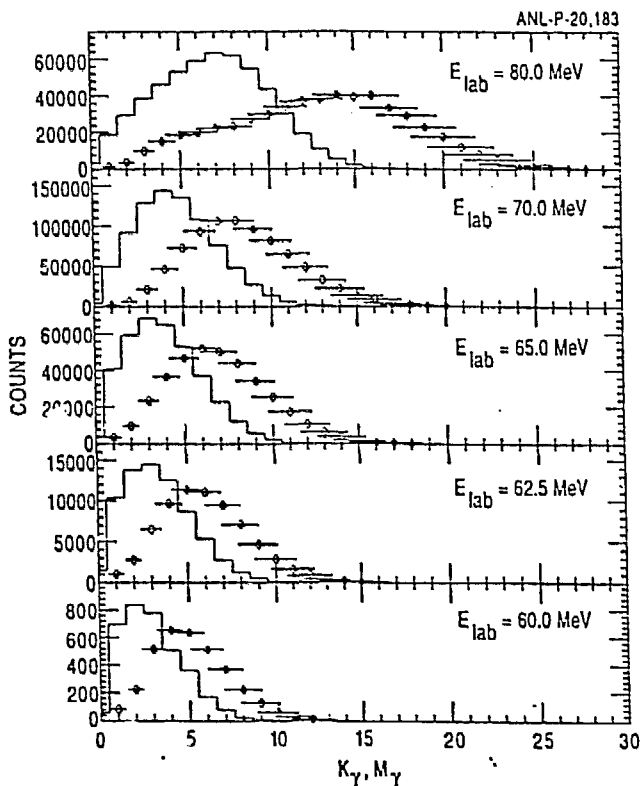


Fig. 11. Fold (histograms) and multiplicity (diamonds) distributions for $^{16}\text{O} + ^{152}\text{Sm}$ fusion as a function of bombarding energy.

distributions were converted to multiplicity distributions using an iterative Monte-Carlo procedure. The resulting multiplicity distributions are also shown in Fig. 1. It is clear that, in the present case, suppression of low folds would severely distort the measured fold distributions and consequently affect the deduced multiplicity distributions.

In order to compare these data with model predictions we have chosen to model the transformation of the theoretical spin distributions to gamma-ray multiplicities as this is conveniently done using existing statistical codes. The angular momentum and excitation energy dependence of the relation between multiplicity and spin is thereby automatically incorporated. The calculations were carried out using the code PACE2S with theoretical spin distributions from either coupled-channels or energy-dependent barrier calculations. Further details are given in Ref. 17. The energy dependence of the cross-section for fusion and moments of the multiplicity distributions are given in Fig. 12 in comparison with the results of the model calculations. The multiplicity data clearly favor the full coupled-channels results over those of the energy-dependent barrier although both give an equally good account of the cross-sections.

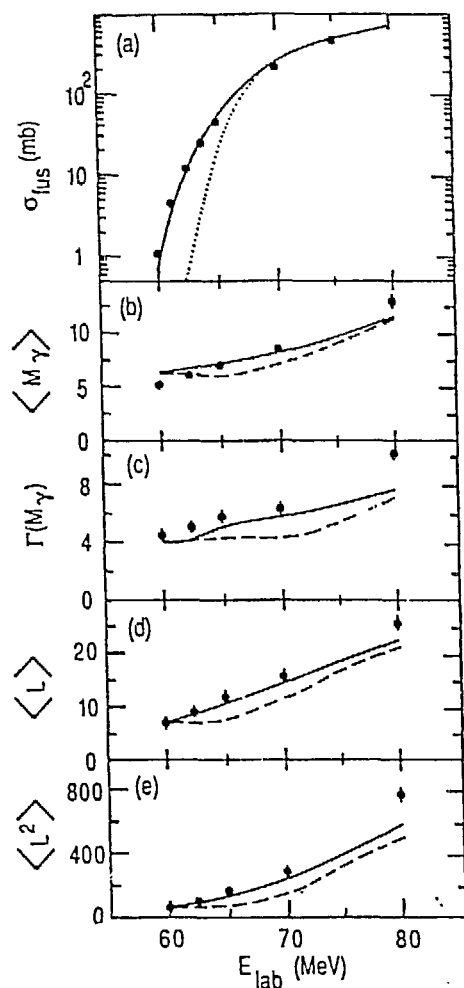


Fig. 12. Cross-sections and moments of multiplicity and spin distributions for $^{16}\text{O} + ^{152}\text{Sm}$ fusion. The results of no-coupling (dots) adjusted-barrier (dashes) and coupled-channels (solid) calculations are shown with the data.

To investigate possible deficiencies in the procedures followed elsewhere whereby multiplicity is converted to spin we have used the code PACE2S to estimate the coefficients in the linear transformation usually used to relate multiplicity and spin. Variation of parameters and input spin distributions produced little variation in the relative numbers of non-statistical and statistical gamma-rays and the numbers of neutrons and charged particles, the resulting mean spin obtained differing by less than 8% in the near barrier region. The moments of the spin distributions thus obtained are shown in Fig. 12 - again showing good agreement with the coupled channels results rather than with the energy-dependent barrier calculations. Finally, the deduced spin distributions are shown in Fig. 13 together with both sets of calculations. The level of agreement with the coupled-channels calculations, particularly in the barrier region, is impressive.

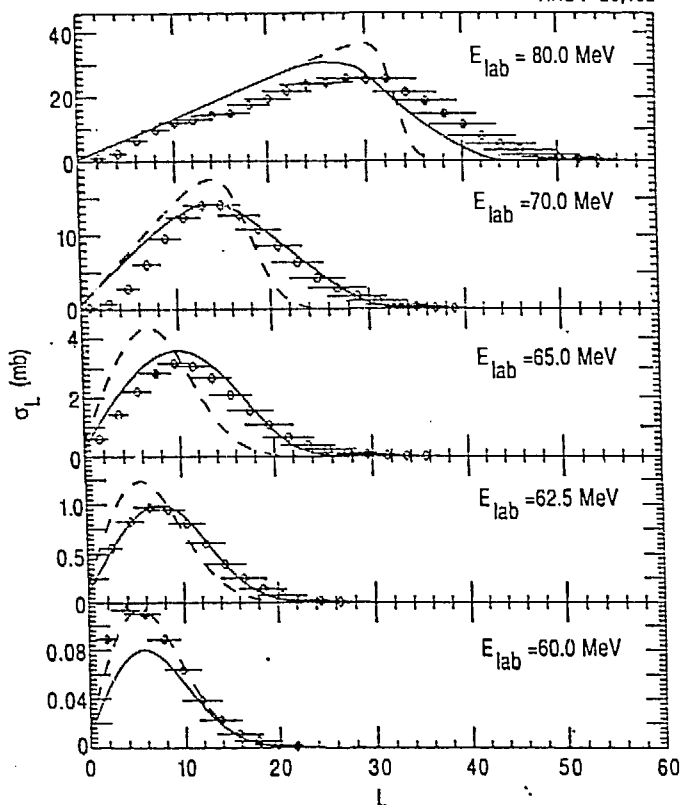


Fig. 13. Spin distributions for $^{16}\text{O} + ^{152}\text{Sm}$ at various bombarding energies. The curves are the results of adjusted-barrier (dashes) and coupled-channels (solid) calculations.

Returning to the critical questions raised regarding the $^{64}\text{Ni} + ^{100}\text{Mo}$ and $^{80}\text{Se} + ^{80}\text{Se}$ data. It seems unlikely that the multiplicity to spin transformation is a problem, especially as the compound system ^{164}Yb is quite close to that studied in detail above. The suppression of low folds may distort the spin distribution somewhat but, as the angular momenta involved are higher than in the $^{16}\text{O} + ^{152}\text{Sm}$ case, the effects should be smaller than would be the case for a lighter projectile. Last, the use of discrete lines to generate the complete multiplicity distribution has been checked with our data by forming multiplicity distributions gated on discrete lines. The resulting distributions were not significantly different. We therefore conclude that the observed extremely high values of the average spin from the $^{64}\text{Ni} + ^{100}\text{Mo}$ and $^{80}\text{Se} + ^{80}\text{Se}$ are indeed real and therefore represent a real challenge in our understanding of low energy fusion.

Fission Angular Distributions: According to the transition-state model of fission, the anisotropy of the fission-fragment angular distribution can, under some assumptions, be related to the mean-square angular momentum of the fissioning system. The only parameters which then enter into this determination are related to the moments of inertia of the saddle-point shape and the nuclear temperature. This model has been used to investigate¹⁸ the spin

distributions of a number of fissioning systems. The results of these analyses are given in Fig. 14. Uniformly, the experimental

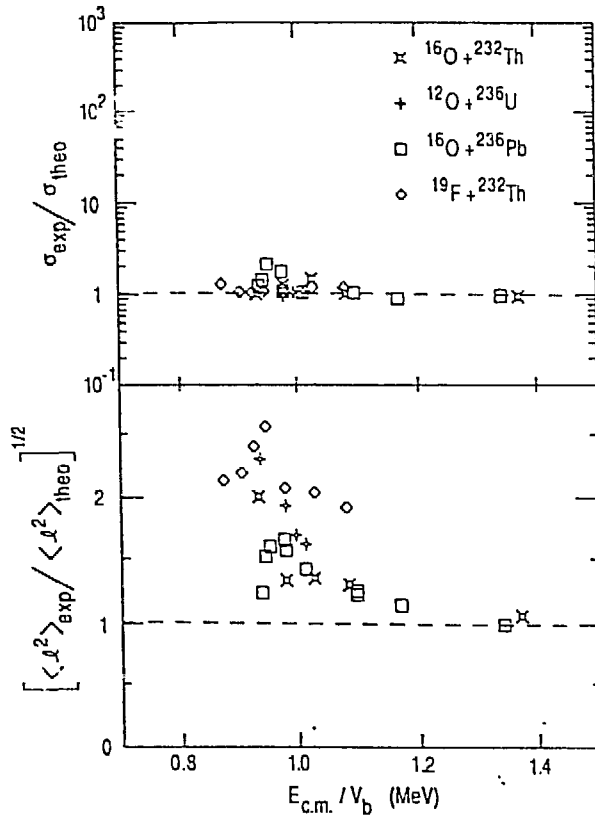


Fig. 14. Comparison of experimental and theoretical cross-sections and average angular momenta deduced from measured fission fragment angular distributions.

spin values are too high as compared to the coupled channels predictions. The question therefore arises again - is this a real discrepancy or some deficiency in the experiment and analysis? Experimentally, it has been suggested that the fission yields can be contaminated by fission occurring following transfer reactions. This has been studied experimentally¹⁹ in the case of $^{16}\text{O} + ^{232}\text{Th}$ and, although present, the transfer fission was not found to be responsible for the observed effects at low energies.

Taking another point of view, the success of the coupled channels formalism in describing spin distributions in fusion of ^{16}O etc. on quite deformed targets must make it improbable that it is the theory that is at fault in the case of these fissioning systems - more likely is our model of the mechanism responsible for the production of the fission fragments.

Anomalously large fission fragment anisotropies are well known. In the case of projectiles incident on targets such that the fissioning system no longer has a fission barrier, large anisotropies were measured even though the standard fission models would predict isotropy²⁰. Further study identified the responsible process as "fast-fission" in which dissipative processes outside the entrance channel barrier produced a damped rotating complex which

subsequently reseparates into fission-like fragments. It has been usually thought that this process would not occur for projectiles as light as ^{16}O . Nevertheless, it is possible that, at sub-barrier energies, such processes may occur even for light projectiles. It is problematic to think of how this question might be further investigated. One possible avenue might be a precise study of the mass and energy distributions of the fission fragments which show the large anisotropies, with the hope that these might be different from fragments produced in "normal" fission. More work is needed to resolve this discrepancy.

SUMMARY

The current status of the experimental study of sub-barrier fusion of heavy ions has been reviewed. For not too heavy systems both the sub-barrier cross-sections and compound nuclear spin distributions are very well described by coupled channels calculations which include coupling to inelastic and transfer degrees of freedom. For heavier, more symmetric, systems similar calculations are unable to describe either the cross-sections or the large values of the average spin of the fused system. This discrepancy thus provides a very real challenge to our understanding of heavy ion reaction dynamics in the sub-barrier region. The uncovering of the degrees of freedom responsible for the additional enhancements and their incorporation in a consistent theory of heavy ion interactions will therefore be a focus of effort in the coming period.

REFERENCES

1. R. G. Stokstad et al. Phys. Rev. Lett. 41, 465 (1978).
2. M. Beckerman et al. Phys. Rev. Lett. 45, 1472 (1980).
3. D. E. DiGregorio et al. Phys. Lett. 176, 322 (1986).
4. C. Wong, Phys. Rev. Lett. 31, 766 (1973).
5. H. Esbensen and S. Landowne, Phys. Rev. C35, 2090 (1987).
6. H. Esbensen and S. Landowne, Nucl. Phys. A492, 473 (1989).
7. K. E. Rehm et al. Phys. Rev. Lett. 55, 280 (1985).
8. J. G. Keller et al. Nucl. Phys. A452, 173 (1986).
9. D. Berdichevsky et al. in Proceedings of Workshop on Nuclear Structure and Heavy Ion Reaction Dynamics, Notre Dame May 26-30, 1990 ed R. R. Betts and J. J. Kolata (IOP, Bristol, 1991) p. 105.
10. M. A. Nagarajan and G. R. Satchler, Phys. Lett. 173B, 29 (1986).
11. C. H. Dasso et al. Phys. Lett. 217B, 25 (1989).
12. D. E. DiGregorio and R. G. Stokstad, Phys. Rev. C43, 265 (1991).
13. S. Gil et al. Phys. Rev. C31, 1752 (1985).
14. S. Gil et al. Phys. Rev. Lett. 65, 3100 (1990).
15. P. J. Nolan et al. Phys. Rev. Lett. 54, 2211 (1985).
16. M. L. Halbert et al. Phys. Rev. C40, 2558 (1989).
17. A. H. Wuosmaa et al. Phys. Lett. (in press).
18. R. Vandenbosch et al. Phys. Rev. Lett. 57, 1499 (1987).
19. B. B. Back et al. in Proceedings of Sixth Winter Workshop on Nuclear Dynamics, Jackson Hole, February 17-24, 1990.
20. B. B. Back et al. Phys. Rev. Lett. 50, 818 (1983).

*Work supported by the U.S. Department of Energy, Nuclear Physics Division, under contract W-31-109-ENG-38.